



Direct evidence for shock-powered optical emission in a nova

Elias Aydi¹✉, Kirill V. Sokolovsky^{1,2}✉, Laura Chomiuk¹✉, Elad Steinberg^{3,4}, Kwan Lok Li^{5,6}, Indrek Vurm⁷, Brian D. Metzger³, Jay Strader¹, Koji Mukai^{8,9}, Ondřej Pejcha¹⁰, Ken J. Shen¹¹, Gregg A. Wade¹², Rainer Kuschnig¹³, Anthony F. J. Moffat¹⁴, Herbert Pablo¹⁵, Andrzej Pigulski¹⁶, Adam Popowicz¹⁷, Werner Weiss¹⁸, Konstanze Zwintz¹⁹, Luca Izzo²⁰, Karen R. Pollard²¹, Gerald Handler²², Stuart D. Ryder²³, Miroslav D. Filipović²⁴, Rami Z. E. Alsaberi²⁴, Perica Manojlović²⁴, Raimundo Lopes de Oliveira^{25,26}, Frederick M. Walter²⁷, Patrick J. Vallely²⁸, David A. H. Buckley²⁹, Michael J. I. Brown³⁰, Eamonn J. Harvey³¹, Adam Kawash¹, Alexei Kniazev^{29,32,33}, Christopher S. Kochanek²⁸, Justin Linford^{34,35,36}, Joanna Mikolajewska²², Paolo Molaro³⁷, Marina Orio^{38,39}, Kim L. Page⁴⁰, Benjamin J. Shappee⁴¹ and Jennifer L. Sokolski³

Classical novae are thermonuclear explosions that occur on the surfaces of white dwarf stars in interacting binary systems¹. It has long been thought that the luminosity of classical novae is powered by continued nuclear burning on the surface of the white dwarf after the initial runaway². However, recent observations of gigaelectronvolt γ -rays from classical novae have hinted that shocks internal to the nova ejecta may dominate the nova emission. Shocks have also been suggested to power the luminosity of events as diverse as stellar mergers³, supernovae⁴ and tidal disruption events⁵, but observational confirmation has been lacking. Here we report simultaneous space-based optical and γ -ray observations of the 2018 nova V906 Carinae (ASASSN-18fv), revealing a remarkable series of distinct correlated flares in both bands. The optical and γ -ray flares occur simultaneously, implying a

common origin in shocks. During the flares, the nova luminosity doubles, implying that the bulk of the luminosity is shock powered. Furthermore, we detect concurrent but weak X-ray emission from deeply embedded shocks, confirming that the shock power does not appear in the X-ray band and supporting its emergence at longer wavelengths. Our data, spanning the spectrum from radio to γ -ray, provide direct evidence that shocks can power substantial luminosity in classical novae and other optical transients.

In a classical nova, the accreted envelope¹ (mass 10^{-7} – $10^{-3} M_{\odot}$) expands and is ejected at velocities of ~ 500 – $5,000$ km s⁻¹. The result is an optical transient where the luminosity of the system increases by a factor of $\sim 10^3$ – 10^6 , sometimes making the source visible to the naked eye⁶. After the initial ejection of the envelope, residual nuclear burning continues on the surface of the hot white dwarf, leading

¹Center for Data Intensive and Time Domain Astronomy, Department of Physics and Astronomy, Michigan State University, East Lansing, MI, USA.

²Astro Space Center of Lebedev Physical Institute, Moscow, Russia. ³Columbia Astrophysics Laboratory and Department of Physics, Columbia University, New York, NY, US. ⁴Racah Institute of Physics, Hebrew University, Jerusalem, Israel. ⁵Department of Physics, UNIST, Ulsan, Korea.

⁶Institute of Astronomy, National Tsing Hua University, Hsinchu, Taiwan. ⁷Tartu Observatory, University of Tartu, Tartumaa, Estonia. ⁸CRESST and X-ray Astrophysics Laboratory, NASA/GSFC, Greenbelt, MD, USA. ⁹Department of Physics, University of Maryland, Baltimore, MD, USA. ¹⁰Institute of Theoretical Physics, Faculty of Mathematics and Physics, Charles University, Prague, Czech Republic. ¹¹Department of Astronomy and Theoretical Astrophysics Center, University of California, Berkeley, Berkeley, CA, US. ¹²Department of Physics and Space Science, Royal Military College of Canada, Kingston, Ontario, Canada. ¹³Institute of Communication Networks and Satellite Communications, Graz University of Technology, Graz, Austria. ¹⁴Département de physique, Université de Montréal, and Centre de Recherche en Astrophysique du Québec, Montréal, Quebec, Canada.

¹⁵AAVSO, Cambridge, MA, USA. ¹⁶Instytut Astronomiczny, Uniwersytet Wrocławski, Wrocław, Poland. ¹⁷Silesian University of Technology, Institute of Electronics, Gliwice, Poland. ¹⁸Institute for Astrophysics, University of Vienna, Vienna, Austria. ¹⁹Universität Innsbruck, Institut für Astro- und Teilchenphysik, Innsbruck, Austria. ²⁰DARK, Niels Bohr Institute, University of Copenhagen, Copenhagen, Denmark. ²¹School of Physical and Chemical Sciences, University of Canterbury, Christchurch, New Zealand. ²²Nicolaus Copernicus Astronomical Center, Polish Academy of Sciences, Warsaw, Poland. ²³Department of Physics and Astronomy, Macquarie University, Sydney, New South Wales, Australia. ²⁴School of Computing Engineering and Mathematics, Western Sydney University, Penrith, New South Wales, Australia. ²⁵Departamento de Física, Universidade Federal de Sergipe, São Cristóvão, Brazil. ²⁶Observatório Nacional, Rio de Janeiro, Brazil. ²⁷Department of Physics and Astronomy, Stony Brook University, Stony Brook, NY, USA. ²⁸Department of Astronomy, The Ohio State University, Columbus, OH, USA. ²⁹South African Astronomical Observatory, Observatory, South Africa. ³⁰School of Physics and Monash Centre for Astrophysics, Monash University, Clayton, Victoria, Australia. ³¹Astrophysics Research Institute, Liverpool John Moores University, Liverpool, UK. ³²Southern African Large Telescope Foundation, Observatory, South Africa. ³³Sternberg Astronomical Institute, Lomonosov Moscow State University, Moscow, Russia. ³⁴Department of Physics and Astronomy, West Virginia University, Morgantown, WV, USA. ³⁵Center for Gravitational Waves and Cosmology, West Virginia University, Morgantown, WV, USA. ³⁶National Radio Astronomy Observatory, Socorro, NM, USA. ³⁷INAF-Osservatorio Astronomico di Trieste, Trieste, Italy. ³⁸INAF-Osservatorio di Padova, Padova, Italy. ³⁹Department of Astronomy, University of Wisconsin, Madison, WI, USA. ⁴⁰School of Physics and Astronomy, University of Leicester, Leicester, UK. ⁴¹Institute for Astronomy, University of Hawai'i, Honolulu, HI, USA. ✉e-mail: aydielia@msu.edu; kirx@kirx.net; chomiuk@msu.edu

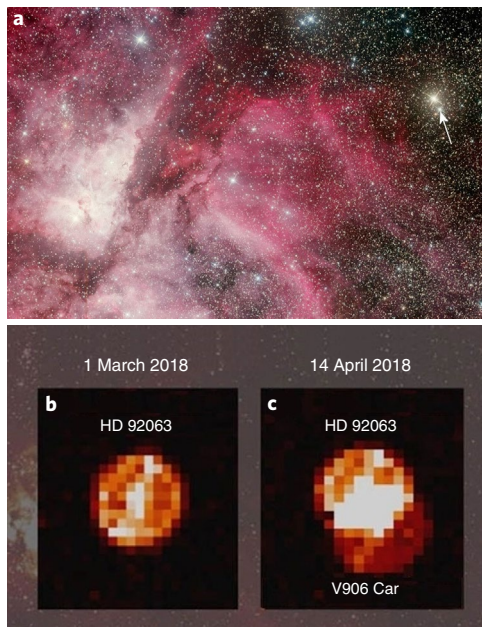


Fig. 1 | Nova V906 Car was discovered in a complex region of the Galaxy near the Carina nebula and the red giant star HD 92063, which was being monitored by the BRITE satellite constellation. **a**, V906 Car pictured in outburst and marked by a white arrow. HD 92063 is the brighter nearby star. **b**, BRITE image from before the outburst of V906 Car taken on 1 March 2018, showing only HD 29063. **c**, BRITE image during the outburst taken on 14 April 2018, showing both HD 92063 and V906 Car. Credit: A. Maury and J. Fabrega (a).

to a phase of quasi-constant, near-Eddington luminosity powered by the hot white dwarf^{2,7}. This should manifest as an optical light curve smoothly declining from maximum light, as the photosphere recedes and the peak of the spectral energy distribution moves blueward from the optical into the ultraviolet and finally into the soft X-ray¹. However, some novae show erratic flares around maximum light with a variety of timescales and amplitudes⁸; these features are still poorly explored and their origin remains a matter of debate. Proposed explanations include instabilities in the envelope of the white dwarf leading to multiple ejection episodes^{9,10}, instabilities in an accretion disk that survived the eruption¹¹ and variations in mass transfer from the secondary to the white dwarf¹².

The optical transient V906 Carinae (ASASSN-18fv) was discovered by the All-Sky Automated Survey for Supernovae (ASAS-SN¹³) on 2018 March 20.3 UT, and was shortly thereafter spectroscopically confirmed as a classical nova^{14,15}. Serendipitously, V906 Car happened to occur in a field being monitored by the BRiGht Target Explorer (BRITE) nanosatellite constellation¹⁶ (Fig. 1), resulting in an unprecedented optical light curve tracking the evolution of the eruption from its start (2018 March 16.13 UT; Fig. 2). The continuous, high-cadence BRITE optical light curve (presented with 1.6 h resolution in Fig. 2, the orbital period of the satellite) revealed a series of eight post-maximum flares during the first month of the outburst, each lasting ~1–3 d with amplitudes $\lesssim 0.8$ mag (Fig. 2; for more details see Methods and the Supplementary Information). Typically, novae are observed using ground-based instruments at lower cadence, and light curves often contain substantial gaps, implying that such short timescale variability would be difficult to resolve.

V906 Car was detected in gigaelectronvolt (GeV) γ -rays around 23 d after eruption by the Large Area Telescope (LAT) on the Fermi Gamma-Ray Space Telescope. The γ -rays persisted at least until day 46 after eruption¹⁷ (Fig. 2). The start time of the γ -ray emission is unconstrained, as the LAT was offline during the first 23 d

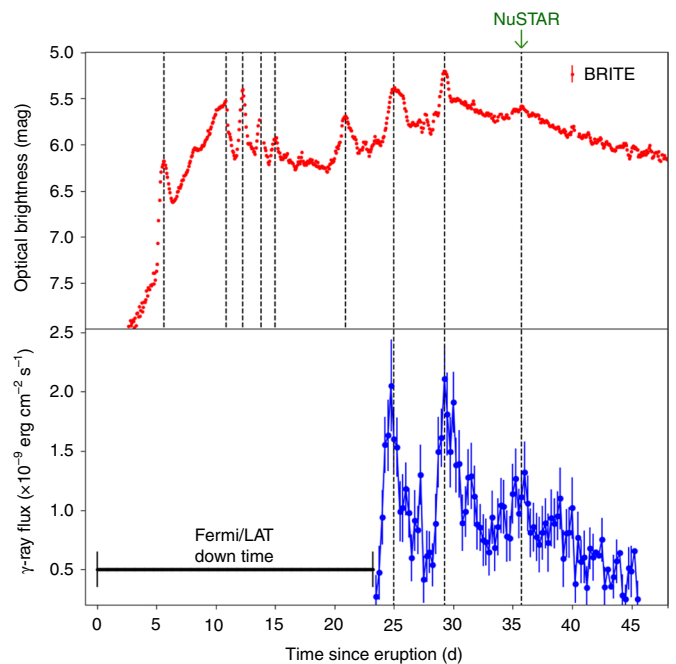


Fig. 2 | The optical and GeV γ -ray light curves of nova V906 Car are correlated, showing simultaneous flares in both bands. The black dashed lines represent the dates of the post-maximum flares. The green arrow indicates the date of the first NuSTAR X-ray observation. The black solid bar indicates the period of Fermi/LAT down time due to technical issues. Fermi entered another observing gap between days 46 and 57. The error bars in the BRITE light curve are 1σ uncertainties. The point-to-point scatter of the binned BRITE measurements is ~ 2 mmag and therefore the size of the error bars is smaller than the symbol size. The error bars in the Fermi light curve are 1σ uncertainties. The eruption start is on 2018 March 16.03 UT (see Methods for more details).

of the eruption. The GeV γ -ray flux reached $2.1 \times 10^{-9} \text{ erg cm}^{-2} \text{ s}^{-1}$ on days 25 and 29, making V906 Car the brightest γ -ray nova to date^{18,19}. Current theory suggests that the GeV γ -rays originate from shocks internal to the nova ejecta—specifically as a fast biconical wind slams into a slower equatorial torus^{20,21}. The shocks accelerate particles to relativistic speeds and γ -rays are produced when these relativistic particles interact with either the surrounding medium or seed photons^{22,23}.

The exceptional γ -ray brightness of V906 Car allowed us to obtain the most detailed γ -ray light curve of a nova to date, showing multiple γ -ray peaks. Comparing this with the BRITE light curve, we see that the γ -ray peaks coincide in time with the optical flares (Fig. 2). This correlation implies that the optical and γ -ray emission in novae share a common origin¹⁹. One possibility is that the luminosity in both bands is driven by shock power—much as has been theorized to occur in type II_n supernovae²⁴. The typical expansion velocities of nova ejecta ($\sim 1,000 \text{ km s}^{-1}$) and timing of the γ -rays (roughly weeks after outburst) imply that the shocked material must have high densities²¹ ($\sim 10^{10} \text{ cm}^{-3}$). At these densities, shocks are expected to be radiative²¹ (that is, the bulk of the shock energy emerges as radiation). Shocks of $\gtrsim 1,000 \text{ km s}^{-1}$ heat gas to $\gtrsim 10^7 \text{ K}$, and therefore typically emit thermal X-rays²⁵. However, at the high densities in nova shocks, the X-ray emission is likely attenuated and/or reprocessed into lower-energy radiation, possibly due to a combination of efficient absorption²¹ and X-ray suppression in corrugated shock fronts²⁶—and therefore the bulk of the shock luminosity may emerge as optical/infrared light.

The observed γ -ray luminosity L_γ of around a few $\times 10^{36} (d/4 \text{ kpc})^2 \text{ erg s}^{-1}$ in V906 Car, implies an energetic shock (we

assume a distance $d = 4.0 \pm 1.5$ kpc to the nova; Supplementary Section 1). Typically, only a few percent of the shock energy goes into the acceleration of relativistic particles²⁷, and ~20% of this energy is emitted in the Fermi/LAT pass-band²¹. Therefore, the kinetic power of the shock is required to be $\geq 10^{38}$ erg s⁻¹—implying that the shock luminosity in V906 Car rivals the bolometric luminosity of the nova (around a few 10^{38} erg s⁻¹; Supplementary Section 5) and likely outstrips the radiative luminosity from the nuclear-burning white dwarf ($\sim 10^{38}$ erg s⁻¹, which is \sim the Eddington Luminosity L_{Edd} for a $1 M_{\odot}$ white dwarf). Meanwhile, the optical- γ -ray correlation implies that the two wavebands share a common source—shocks—and therefore that shock luminosity is emerging in the optical band. This challenges the standard paradigm, which attributes the bolometric luminosity of novae to thermal energy from the white dwarf.

We can test where in the electromagnetic spectrum the shock luminosity emerges using X-ray observations concurrent with the γ -ray detections. Softer X-rays (<10 keV) are usually not detected while novae are observed to emit γ -rays^{21,28}, and V906 Car is no exception. The X-ray Telescope (XRT) on the Neil Gehrels Swift Observatory monitored V906 Car during the γ -ray emission on days 5 and 37, but no X-rays were detected in the 0.3–10.0 keV range with a 3σ upper limit on the observed luminosity, $L_{\text{X}} < 4 \times 10^{33} (d/4 \text{ kpc})^2 \text{ erg s}^{-1}$. However, these observations cannot rule out the presence of luminous, but heavily absorbed, X-ray emission. On day 36, coinciding with the last optical/ γ -ray flare, we detected harder (3.5–78.0 keV) X-rays from V906 Car with the Nuclear Spectroscopic Telescope Array (NuSTAR) satellite (Methods). The detected X-rays were consistent with a highly absorbed ($N_{\text{H}} = 1.9 \times 10^{23} \text{ cm}^{-2}$, where N_{H} is the column density) thermal plasma with an unabsorbed luminosity of $L_{\text{X}} = (2.4 \pm 0.2) \times 10^{34} (d/4 \text{ kpc})^2 \text{ erg s}^{-1}$ (Supplementary Section 5). Therefore, the GeV γ -ray luminosity of V906 Car is a factor of ~ 300 higher than the hard X-ray luminosity. This L_{X}/L_{γ} is consistent with theoretical predictions of heavy absorption and X-ray suppression in nova shocks²⁶, and indicates that the majority of the shock luminosity is indeed emitted in the optical band.

An alternative explanation for the optical- γ -ray correlation in V906 Car is if the particle acceleration were very efficient (>10%) and variations in luminosity of the binary (perhaps on the white dwarf surface or in the accretion disk) power the flares in the optical light curve. These luminosity variations would lead to time-variable, radiation-driven outflows which in turn produce shocks and γ -rays. In this case, the γ -ray flares should lag the optical flares in time (possibly by several days; Supplementary Section 6). The unprecedented optical and γ -ray light curves of V906 Car enable us to test for any time lag between the optical and γ -ray emission—something that has never been possible for a nova previously. Our correlation analysis (Supplementary Section 4) implies that the γ -ray emission precedes the optical by $\sim 5.3 \pm 2.7$ h (2σ significance). We can also rule out that the γ -rays lag the optical by more than 2.5 h at 3σ significance. The optical and γ -ray light curves of V906 Car are thus inconsistent with thermal emission from the white dwarf, and provide strong evidence for shocks powering the optical flares.

Our high-resolution optical spectra (Supplementary Section 2) and light curves lead us to suggest the following scenario for V906 Car. A dense slowly expanding torus (with an expansion velocity $v_1 < 600 \text{ km s}^{-1}$) is ejected in the binary's orbital plane during the first days of the eruption²⁰. This torus has a complex density structure, consisting perhaps of a spiral or multiple shells²⁹. Later, a fast wind develops with expansion velocity, $v_2 \approx 1,200 \text{ km s}^{-1}$, and shocks the torus, presumably leading to γ -rays and other shock-powered emission. The first four optical flares are created when the wind slams into the higher density structures in the torus, leading to temporary increases in the output shock luminosity. Around 20 d after the eruption, we witness an even faster wind emerging ($v_3 \approx 2,500 \text{ km s}^{-1}$; Supplementary Section 2). The faster wind slams into the torus, which is now merged with the previous wind, leading to the second

sequence of the optical and correlated γ -ray flares (between 22 and 36 d after eruption). This multiple-ejection scenario is supported by our radio light curve of V906 Car, which is consistent with a delayed expansion of the bulk of the ejecta (~ 10 – 20 d after eruption) and is not consistent with a single homologous ejection (Supplementary Section 3). While this scenario might be unique to V906 Car given the diversity of nova observations⁶, it supports a general unified picture in which a substantial fraction of nova emission is radiated by internal shocks. The correlation also suggests that the long-debated flares seen in the optical light curves of some novae are originating from shock interactions.

The timescales and luminosities of other optical transients, such as type II_n, Ia-CSM (CircumStellar Medium) and superluminous supernovae, have led to the conclusion that these events are shock powered—that is, the bulk of their bolometric luminosity originates as X-rays from shocks that are then absorbed and reprocessed to emerge in the optical^{4,30,31}. Similar suggestions have been made for luminous red novae³, stellar mergers and tidal disruption events⁵. Shocks are often theorized as a flexible way to power the most luminous transients in the sky^{32,33}. However, there has never been direct evidence for shocks dominating the bulk of the bolometric luminosity of transients. Our observations of nova V906 Car definitively demonstrate that substantial luminosity can be produced—and emerge at optical wavelengths—by heavily absorbed, energetic shocks in explosive transients. They also show that these same shocks can accelerate charged particles to relativistic speeds, implying that shock-powered supernovae may be important sources of cosmic rays^{34,35}. With modern time-domain surveys such as ASAS-SN, the Zwicky Transient Facility (ZTF) and the Vera C. Rubin Observatory, we will be discovering more—and higher luminosity—transients than ever before. The novae in our galactic backyard will remain critical for testing the physical drivers powering these distant, exotic events.

Methods

The ASAS-SN discovery. V906 Car (ASASSN-18fv) was first discovered as a possible, bright galactic nova by the ASAS-SN^{13,36} on 2018 March 20.3 UT¹⁴ with $V < 10$ mag (saturated). The nova is located at J2000.0 equatorial coordinates of $(\alpha, \delta) = (10 \text{ h } 36 \text{ min } 15.42 \text{ s}, -59^{\circ} 35' 54.0'')$ and galactic coordinates of $(l, b) = (286.580^{\circ}, -1.088^{\circ})$; see ref. ¹⁴). Shortly thereafter, the transient was confirmed spectroscopically as a classical nova¹⁵. Pre-discovery observations obtained using Evryscope-South³⁷ and BRITe suggest that the eruption started on 2018 March 16.13 UT. Therefore, we will assume this date as the eruption start (t_0).

BRITe photometry. On 20 February 2018, one of the five BRITe Constellation^{16,38} satellites, BRITe-Toronto (BTr), started observations of 18 stars in the Carina field. Among those preselected objects was the red giant HD 92063 (K1 III, $V = 5.08$ mag). The instrument aboard BTr is a five-lens, 3-cm-aperture telescope feeding an uncooled CCD (charge-coupled device). BTr is also equipped with a red filter transmitting light between 550 and 700 nm. The pixel size of the BRITe CCD detector (KAI-11002M) is $9 \mu\text{m}$ and the image scale is 27 arcsec per pixel.

The exposure time was set to 4 s and images were taken every 20 s. The observations were obtained over 16 min during each 98.24 min satellite orbit. Until 18 March 2018, no notable variability of HD 92063 was apparent in the BRITe photometry outside the 2 mmag root-mean-squared scatter. A few days later, on 22 March 2018, an upward trend in brightness was clearly noticeable. An inspection of the images of HD 92063 revealed that another object appeared close to, in fact merging with, the point-spread function (full-width at half-maximum ~ 8 pixels or 3.6 arcmin) of the target (Fig. 1). This new source was discovered by ASAS-SN as ASASSN-18fv (V906 Car) and soon thereafter classified as a classical nova.

The observations of the nova were reduced with the standard BRITe pipeline³⁹, which provides aperture photometry. The raw BRITe photometry was subsequently processed to remove instrumental effects following the procedure outlined by ref. ⁴⁰. The procedure includes rejection of outliers and the worst orbits, and decorrelation of instrumental effect like CCD temperature and orbital phase.

γ -ray observations and analysis. The GeV γ -ray detection of V906 Car was first reported in ref. ¹⁷. According to the preliminary report, γ -ray emission was substantially detected over the period 14–18 April 2018, but no detailed spectral or temporal information of the emission was provided. Here we analyse the Fermi/LAT data to extract the γ -ray light curve and the spectral energy distribution (SED) of V906 Car.

We downloaded the LAT data (pass 8, release 3, version 2 with the instrument response functions of P8R3_SOURCE_V2) from the data server at the Fermi Science Support Center. The observations cover the period of 8–30 April 2018. We intended to use a broader time coverage; however, no LAT observations were performed for the region of interest (ROI) during 17 March–7 April and 01–12 May due to a solar panel issue on Fermi.

The data reduction and analyses were all performed using *fermitools* (version 1.0.5) with *fermitools-data* (version 0.17), which can be found at <https://fermi.gsfc.nasa.gov/ssc/data/analysis/software/>. For data selection, an ROI of $14^\circ \times 14^\circ$ centred on the nova was used. Events with the class *evclass*=128 (that is, SOURCE class) and the type *evtype*=3 (that is, reconstructed tracks FRONT and BACK) were selected. We excluded events with zenith angles larger than 90° to avoid contamination from the Earth's limb. The selected events also had to be taken during good time intervals, which fulfils the *gtmtime* filter (*DATA_QUAL* > 0) && (*LAT_CONFIG*==1).

We then performed binned likelihood analysis on the selected LAT data. A γ -ray emission model for the whole ROI was built using all of the fourth Fermi/LAT catalog (4FGL) catalogued sources⁴¹ located within 20° of the nova. As V906 Car was the brightest γ -ray source in the field and its emission dominated within a 2° radius, we simply fixed all the spectral parameters of the field sources to the values in 4FGL to save computational time. In addition, the galactic diffuse emission and the extragalactic isotropic diffuse emission were included by using the pass 8 background models *gll_iem_v07.fits* and *iso_P8R3_SOURCE_V2_v1.txt*, respectively, which were allowed to vary during the fitting process.

Given the spectral curvature of V906 Car (see the SED in Supplementary Fig. 17), we considered two spectral models: a power law with an exponential cutoff, *PLExpCutoff*

$$\frac{dN}{dE} \propto E^{-\Gamma} \exp\left(-\frac{E}{E_c}\right)$$

characterized by a photon index Γ and energy cutoff E_c (we find photon flux $F_{\text{ph},\gamma} = 1.22 \pm 0.04 \text{ ph cm}^{-2} \text{ s}^{-1}$, $E_c = 5.9 \pm 1.1 \text{ GeV}$ and $\Gamma = 1.76 \pm 0.05$, with Test Statistic $\text{TS} = 3,591$), where N is number of photons, and E is the photon energy; and a logarithmic power law, *LogParabola*:

$$\frac{dN}{dE} \propto \left(\frac{E}{E_b}\right)^{-(\Gamma + \beta \log(E/E_b))}$$

where β defines the degree of curvature and $E_b = 100 \text{ MeV}$ is a fixed scale parameter. Both models can fit the data reasonably well. Formally, *LogParabola* performs better with $\Delta \text{TS} \approx 57$, so we used it as our standard model. The best-fit spectral parameters of the *LogParabola* fit to the full dataset are $\Gamma = 1.14 \pm 0.09$, $\beta = 0.21 \pm 0.02$ and photon flux $F_{\text{ph}}(0.1\text{--}300 \text{ GeV}) = (1.04 \pm 0.04) \times 10^{-6} \text{ photons cm}^{-2} \text{ s}^{-1}$ with $\text{TS} = 3,649$.

We extracted the γ -ray light curve for 0.1–300 GeV using the *LogParabola* model with Γ and β fixed to their best-fit values (only the normalization was allowed to vary). Several binning factors were tried and we finally used 6 h bins as a good balance between the temporal resolution and the noise level of each bin (Fig. 2). The nova was significantly (greater than 5σ significance) detected in most of the bins and 95% upper limits were computed for bins with $\text{TS} < 4$.

We also extracted a ten bin SED of V906 Car using geometric binning. To make the SED less model dependent, we used a simple power-law model of $\Gamma = 2$ (fixed; which is flat for a νF_ν -based SED, where ν is the frequency and F_ν is the flux density) to model the energy in each bin. As V906 Car is undetected in the last two bins of the SED (that is, $\text{TS} \approx 0$), we combined them to compute a 95% upper limit. The final SED is shown in Supplementary Fig. 17.

We fit a simple power law to daily-binned γ -ray data to search for any temporal variation in the energy spectrum. The photon index for the data bins with $\text{TS} > 25$ (that is, significantly detected daily at $>5\sigma$, assuming a simple power law) does not show notable changes. We conclude that there is no strong spectral variability in the data of nova V906 Car. The 1 d cadence light curve and the photon index of the 1 d binned data assuming a power-law fit can be found through this link: <http://scan.sai.msu.ru/~kirx/v906car/>.

X-ray observations with Swift. The XRT on the Neil Gehrels Swift Observatory monitored V906 Car during the optical/ γ -ray flaring. The observations obtained on 21 March 2018 and 22 April 2018, of 1 ks and 1.25 ks exposures, respectively, led to a non-detection in the 0.3–10.0 keV X-ray range with a 3σ upper limit on the observed luminosity, $L_x < 4.4 \times 10^{33} (d/4.0 \text{ kpc})^2 \text{ erg s}^{-1}$. This implies an unabsorbed luminosity $L_x < 1.2 \times 10^{34} (d/4.0 \text{ kpc})^2 \text{ erg s}^{-1}$, assuming a highly absorbed thermal plasma. Supersoft (0.3–1.0 keV) emission was only detected by Swift $>200 \text{ d}$ after the eruption (Sokolovsky et al., manuscript in preparation).

Hard X-ray observations with NuSTAR and XMM-Newton. Owing to its unique optics capable of focusing X-rays in the energy range 3–78 keV, NuSTAR⁴² is two orders of magnitude more sensitive compared with the earlier coded aperture mask instruments operating at this energy range. V906 Car was observed with NuSTAR on 21 April 2018 and 12 May 2018 (36 and 57 d after the eruption). The nova was

still bright in γ -rays during the first NuSTAR observation and no simultaneous Fermi/LAT observations are available during the second NuSTAR epoch. Both NuSTAR observations had integration times of about 48 ks and resulted in highly significant detections (24σ and 42σ , respectively) of the nova. The 3–78 keV spectra lack obvious features such as emission lines or absorption edges and can be fit with an absorbed thermal plasma model, with the temperature decreasing from $8.6 \pm 0.8 \text{ keV}$ in the first epoch to $4.3 \pm 0.2 \text{ keV}$ in the second epoch. To account for the lack of obvious spectral features in the NuSTAR band, we have to assume non-solar metallicities (see below). Specifically, it is puzzling that the NuSTAR spectra show no signs of iron emission and absorption while the optical spectra of the nova reveal strong iron lines. An iron abundance of less than 0.1 solar is required to fit the NuSTAR data. The alternative model that provides a good fit to our NuSTAR data has the iron abundance fixed to the solar value, but requires an overabundance of CNO elements by a factor of 200 over the solar values. The ‘CNO overabundance’ and ‘iron deficiency’ models imply a factor of 70 difference in the total absorbing column, while both models suggest values well in excess of the expected galactic column.

We performed a target of opportunity observation with XMM-Newton on 16 December 2018 (275 d post-explosion) to constrain the abundances in the nova ejecta. The joint analysis of the high-resolution X-ray grating (0.3–2.1 keV) and medium-resolution CCD (0.3–10 keV) XMM-Newton spectra suggests that the iron abundance (by number) is less than 0.1 of the solar value, while the ejecta are enriched with N and O by factors of 350 and 30, respectively. Using these abundance values to fit the NuSTAR spectra, we derive absorbing columns of $N_{\text{H}} = (1.9 \pm 1) \times 10^{23} \text{ cm}^{-2}$ on day 36 and $(2.6 \pm 0.2) \times 10^{22} \text{ cm}^{-2}$ on day 57. The unabsorbed fluxes (extrapolating to the 0.3–78 keV energy range) are $1.3 \times 10^{-11} \text{ erg cm}^{-2} \text{ s}^{-1}$ and $1.6 \times 10^{-11} \text{ erg cm}^{-2} \text{ s}^{-1}$ (statistical uncertainty of $\sim 20\%$) for the two epochs, respectively. A detailed discussion of the X-ray spectroscopy results will be presented by Sokolovsky et al. (manuscript in preparation).

Data availability

The data that support the plots within this paper and other findings of this study are available from <http://scan.sai.msu.ru/~kirx/v906car/> or from the corresponding authors upon reasonable request.

Received: 18 November 2019; Accepted: 25 February 2020;

Published online: 13 April 2020

References

- Bode, M. F. & Evans, A. *Classical Novae* 2nd edn (Cambridge Astrophysics Series No. 43, Cambridge Univ. Press, 2008).
- Gallagher, J. S. & Starrfield, S. Theory and observations of classical novae. *Annu. Rev. Astron. Astrophys.* **16**, 171–214 (1978).
- Metzger, B. D. & Pejcha, O. Shock-powered light curves of luminous red novae as signatures of pre-dynamical mass-loss in stellar mergers. *Mon. Not. R. Astron. Soc.* **471**, 3200–3211 (2017).
- Moriya, T. J., Sorokina, E. I. & Chevalier, R. A. Superluminous supernovae. *Space Sci. Rev.* **214**, 59 (2018).
- Roth, N., Kasen, D., Guillochon, J. & Ramirez-Ruiz, E. The X-ray through optical fluxes and line strengths of tidal disruption events. *Astrophys. J.* **827**, 3 (2016).
- Warner, B. *Cataclysmic Variable Stars* 2nd edn (Cambridge Astrophysics Series No. 28, Cambridge Univ. Press, 1995).
- Wolf, W. M., Bildsten, L., Brooks, J. & Paxton, B. Hydrogen burning on accreting white dwarfs: stability, recurrent novae, and the post-nova supersoft phase. *Astrophys. J.* **777**, 136 (2013).
- Strope, R. J., Schaefer, B. E. & Henden, A. A. Catalog of 93 nova light curves: classification and properties. *Astron. J.* **140**, 34–62 (2010).
- Cassatella, A., Lamers, H. J. G. L. M., Rossi, C., Altamore, A. & González-Riestra, R. A study of the expanding envelope of nova V1974 Cyg 1992 based on IUE high resolution spectroscopy. *Astron. Astrophys.* **420**, 571–588 (2004).
- Hillman, Y., Prialnik, D., Kovetz, A., Shara, M. M. & Neill, J. D. Nova multiwavelength light curves: predicting UV precursor flashes and pre-maximum halts. *Mon. Not. R. Astron. Soc.* **437**, 1962–1975 (2014).
- Goranskij, V. P. et al. Photometric and spectroscopic study of nova Cassiopeiae 1995 (V723 Cas). *Astrophys. Bull.* **62**, 125–146 (2007).
- Chochol, D. & Pribulla, T. Photometric variability of the slow nova V723 Cas. *Contrib. Astron. Obs. Skaln. Pleso* **28**, 121 (1998).
- Shappee, B. J. et al. The man behind the curtain: X-rays drive the UV through NIR variability in the 2013 active galactic nucleus outburst in NGC 2617. *Astrophys. J.* **788**, 48 (2014).
- ASAS-SN Discovery of a possible, very bright galactic nova ASASSN-18fv. *The Astronomer's Telegram* 11454 (2018).
- Lucas, P. Spectroscopic observations of ASASSN-18fv as a classical nova in the iron curtain phase. *The Astronomer's Telegram* 11460 (2018).
- Pablo, H. et al. The BRITe constellation nanosatellite mission: testing, commissioning, and operations. *Publ. Astron. Soc. Pac.* **128**, 125001 (2016).

17. Jean, P., Cheung, C. C., Ojha, R., van Zyl, P. & Angioni, R. Fermi-LAT bright gamma-ray detection of nova ASASSN-18fv. *The Astronomer's Telegram* 11546 (2018).
18. Franckowiak, A., Jean, P., Wood, M., Cheung, C. C. & Buson, S. Search for gamma-ray emission from galactic novae with the Fermi-LAT. *Astron. Astrophys.* **609**, A120 (2018).
19. Li, K.-L. et al. A nova outburst powered by shocks. *Nat. Astron.* **1**, 697–702 (2017).
20. Chomiuk, L. et al. Binary orbits as the driver of γ -ray emission and mass ejection in classical novae. *Nature* **514**, 339–342 (2014).
21. Metzger, B. D. et al. Gamma-ray novae as probes of relativistic particle acceleration at non-relativistic shocks. *Mon. Not. R. Astron. Soc.* **450**, 2739–2748 (2015).
22. Tatischeff, V. & Hernanz, M. Evidence for nonlinear diffusive shock acceleration of cosmic rays in the 2006 outburst of the recurrent nova RS Ophiuchi. *Astrophys. J. Lett.* **663**, 101–104 (2007).
23. Martin, P., Dubus, G., Jean, P., Tatischeff, V. & Dosne, C. Gamma-ray emission from internal shocks in novae. *Mon. Not. R. Astron. Soc.* **612**, A38 (2018).
24. Chugai, N. N. et al. The type II supernova 1994w: evidence for the explosive ejection of a circumstellar envelope. *Mon. Not. R. Astron. Soc.* **352**, 1213–1231 (2004).
25. Slane, P., Bykov, A., Ellison, D. C., Dubner, G. & Castro, D. Supernova remnants interacting with molecular clouds: X-ray and gamma-ray signatures. *Space Sci. Rev.* **188**, 187–210 (2015).
26. Steinberg, E. & Metzger, B. D. The multidimensional structure of radiative shocks: suppressed thermal X-rays and relativistic ion acceleration. *Mon. Not. R. Astron. Soc.* **479**, 687–702 (2018).
27. Caprioli, D. & Spitkovsky, A. Simulations of ion acceleration at non-relativistic shocks. I. Acceleration efficiency. *Astrophys. J.* **783**, 91 (2014).
28. Nelson, T. et al. NuSTAR detection of X-rays concurrent with gamma-rays in the nova V5855 Sgr. *Astrophys. J.* **872**, 86 (2019).
29. Pejcha, O., Metzger, B. D. & Tomida, K. Cool and luminous transients from mass-losing binary stars. *Mon. Not. R. Astron. Soc.* **455**, 4351–4372 (2016).
30. Smith, N. & McCray, R. Shell-shocked diffusion model for the light curve of SN 2006gy. *Astrophys. J. Lett.* **671**, L17–L20 (2007).
31. Silverman, J. M. et al. Type Ia supernovae strongly interacting with their circumstellar medium. *Astrophys. J. Suppl. Ser.* **207**, 3 (2013).
32. Dong, S. et al. ASASSN-15lh: a highly super-luminous supernova. *Science* **351**, 257–260 (2016).
33. Chatzopoulos, E. et al. Extreme supernova models for the super-luminous transient ASASSN-15lh. *Astrophys. J.* **828**, 94 (2016).
34. Murase, K., Thompson, T. A. & Ofek, E. O. Probing cosmic ray ion acceleration with radio-submm and gamma-ray emission from interaction-powered supernovae. *Mon. Not. R. Astron. Soc.* **440**, 2528–2543 (2014).
35. Murase, K., Franckowiak, A., Maeda, K., Margutti, R. & Beacom, J. F. High-energy emission from interacting supernovae: new constraints on cosmic-ray acceleration in dense circumstellar environments. *Astrophys. J.* **874**, 80 (2019).
36. Kochanek, C. S. et al. The All-sky Automated Survey for Supernovae (ASAS-SN) light curve server v1.0. *Publ. Astron. Soc. Pac.* **129**, 104502 (2017).
37. Corbett, H. et al. Pre-discovery detection of ASASSN-18fv by Evryscope. *The Astronomer's Telegram* 11467 (2018).
38. Weiss, W. W. et al. BRITe constellation: nanosatellites for precision photometry of bright stars. *Publ. Astron. Soc. Pac.* **126**, 573 (2014).
39. Popowicz, A. et al. BRITe constellation: data processing and photometry. *Astron. Astrophys.* **605**, A26 (2017).
40. Pigulski, A. BRITe cookbook 2.0. In *3rd BRITe Science Conference* Vol. 8 (eds Wade, G. A. et al.) 175–192 (Polish Astronomical Society, 2018).
41. Abdollahi, S. et al. Fermi Large Area Telescope fourth source catalog. *Astrophys. J. Suppl. Ser.* **247**, 33 (2020).
42. Harrison, F. A. et al. The Nuclear Spectroscopic Telescope Array (NuSTAR) high-energy X-ray mission. *Astrophys. J.* **770**, 103 (2013).

Acknowledgements

E.A., L.C. and K.V.S. acknowledge NSF award AST-1751874, NASA award 11-Fermi 80NSSC18K1746 and a Cottrell fellowship of the Research Corporation. K.L.L. was

supported by the Ministry of Science and Technology of Taiwan through grant 108-2112-M-007-025-MY3. J.S. was supported by the Packard Foundation. O.P. was supported by Horizon 2020 ERC Starting Grant ‘Cat-In-hAT’ (grant agreement number 803158) and INTER-EXCELLENCE grant LTAUSA18093 from the Czech Ministry of Education, Youth, and Sports. Support for K.J.S. was provided by NASA through the Astrophysics Theory Program (NNX17AG28G). G.A.W. acknowledges Discovery Grant support from the Natural Sciences and Engineering Research Council (NSERC) of Canada. A.F.J.M. is grateful for financial assistance from NSERC (Canada) and FQRNT (Quebec). A.Pigulski acknowledges support provided by the Polish National Science Center (NCN) grant No.number 2016/21/B/ST9/01126. A.Popowicz was supported by statutory activities grant SUT 02/010/BKM19 t.20. D.A.H.B. gratefully acknowledge the receipt of research grants from the National Research Foundation (NRF) of South Africa. A.Kniazev acknowledges the National Research Foundation of South Africa and the Russian Science Foundation (project no.14-50-00043). R.K., W.W. and K.Z. acknowledge support from the Austrian Space Application Programme (ASAP) of the Austrian Research Promotion Agency (FFG). I.V. acknowledges the support by the Estonian Research Council grants IUT26-2 and IUT40-2, and by the European Regional Development Fund (TK133). This research has been partly founded by the National Science Centre, Poland, through grant OPUS 2017/27/B/ST9/01940 to J.M. This work is based on data collected by the BRITe Constellation satellite mission, designed, built, launched, operated and supported by the Austrian Research Promotion Agency (FFG), the University of Vienna, the Technical University of Graz, the University of Innsbruck, the Canadian Space Agency (CSA), the University of Toronto Institute for Aerospace Studies (UTIAS), the Foundation for Polish Science and Technology (FNP/MNiSW) and National Science Centre (NCN). G.H. is indebted to the Polish National Science Center for funding by grant number 2015/18/A/ST9/00578. C.S.K. is supported by NSF grants AST-1908952 and AST-1814440. We acknowledge the use of public data from the Swift data archive. UK funding for the Neil Gehrels Swift Observatory is provided by the UK Space Agency. This research has made use of data and/or software provided by the High Energy Astrophysics Science Archive Research Center (HEASARC), which is a service of the Astrophysics Science Division at NASA/GSFC and the High Energy Astrophysics Division of the Smithsonian Astrophysical Observatory. A part of this work is based on observations made with the Southern African Large Telescope (SALT), under the Large science Programme on transient 2018-2-LSP-001. Polish participation in SALT is funded by grant number MNiSW DIR/WK/2016/07. The Australia Telescope Compact Array is part of the Australia Telescope National Facility, which is funded by the Australian Government for operation as a National Facility managed by CSIRO. We acknowledge ARAS observers T. Bohlens, B. Heathcote and P. Luckas for their optical spectroscopic observations which complement our database. Nova research at Stony Brook is supported in part by NSF grant AST 1614113, and by research support from Stony Brook University. We thank E. R. Colmenero for initiating the collaboration that has led to this paper.

Author contributions

E.A. wrote the text. A.Pigulski, A.Popowicz, R.K., K.V.S., L.C., S.R., M.F., R.A., P.Manojlović, R.L.d.O., J.S., K.L.L., A.Kniazev, L.L., F.M.W. and K.R.P. obtained and reduced the data. All authors contributed to the interpretation of the data and commented on the final manuscript.

Competing interests

The authors declare no competing interests.

Additional information

Supplementary information is available for this paper at <https://doi.org/10.1038/s41550-020-1070-y>.

Correspondence and requests for materials should be addressed to E.A., K.V.S. or L.C.

Peer review information *Nature Astronomy* thanks Anna Franckowiak and the other, anonymous, reviewer(s) for their contribution to the peer review of this work.

Reprints and permissions information is available at www.nature.com/reprints.

Publisher's note Springer Nature remains neutral with regard to jurisdictional claims in published maps and institutional affiliations.

© The Author(s), under exclusive licence to Springer Nature Limited 2020